5th ECPMG Delft · 2024

Proceedings of the 5th ECPMG 2024
5th European Conference on Physical Modelling in Geotechnics
2-4 October 2024, Delft, the Netherlands

Assessing combined cyclic axial and lateral performance of a pile installed in calcarenite using the ICE-PICK testing apparatus

T. Riccio
[1]University of Dundee, Dundee, Scotland, 140007677@dundee.ac.uk

Tomas Romero[3], M.O Ciantia[1,2], M Manica[3],
M Previtali[1], M J Brown[1]
[2]Department of Earth and Environmental Sciences, University of Milano Bicocca
[3]Institute of Engineering, National Autonomous University of Mexico, Mexico

ABSTRACT: Small scale experimental tests have been used historically to complement field testing and, more recently, to validate numerical models. In this instance, a novel small-scale multi-axial testing apparatus is presented. This multi-axis frame was developed to study the installation effects on cyclic axial and lateral performance of displacement piles in chalk (ICE-PICK: EP/W00013X/1). The apparatus overcomes some limitations of prior small scale testing apparatus by allowing for simultaneous multi-directional loading due to its 3-axis actuation system. Additionally, it has been designed for compactness, allowing tests to be carried out within an X-ray CT scanning bay, in order to reveal the evolution of soil-structure interaction. Within this scope, a brief overview of the systems construction and performance is given, followed by a demonstration test on pile installation and, subsequently, combined vertical and cyclic lateral loading.

1 INTRODUCTION

Small-scale physical models can be used to study soil and rock-structure interaction problems. These studies are typically designed around separate axial and lateral loading due to loading frame limitations (Lehane and Gavin 2001, Peng et al. 2006, LeBlanc et al. 2010, Roesen et al. 2013, Arshad and O'Kelly 2014), the latter typically addressing characteristics and magnitude of cyclic loading (i.e., one-way, two way or unbalanced) which are critical for offshore wind turbine foundations (Frick and Achmus 2021). Nevertheless, only a few examples consider multi-directional loading (Su 2012, Mayoral et al. 2016). In the case of offshore foundations, such loading characteristics have been found to deteriorate the pile's ultimate lateral capacity, leading to greater accumulated displacement over a lifetime of cyclic loading when compared to uni-directional loading cases (Rudolph and Grabe 2014).

In sensitive materials, such as soft rock, e.g. calcarenite, lateral pile performance may also be significantly affected by the installation procedure. In an offshore environment, piles are typically driven or jacked, and such mechanical action has been shown to cause crushing and pore collapse near to the pile annulus (Ciantia et al. 2021, Zheng et al. 2023), leading to a material which no longer exhibits its stiff elastic properties and rather exhibits a hypo elastic, soil-like behaviour. These effects are marked in the case of soft rock and have been observed to cause poor performance of pile foundations within their serviceable lateral limit (Ciavaglia et al. 2017).

Instrumentation of small-scale models traditionally requires local measurements, which provide useful information in terms of a discrete data stream but often overlook in-situ mechanisms that contribute significantly to the soil-structure response. Using image analysis techniques, such as PIV (Yuan et al.; 2017), allow for a more complete description of the phenomenon at the cost of additional constraints to the modelling operations (i.e. plane-symmetric boundary conditions). To overcome some of these limitations, X-ray computed tomography and radiography has been used by several researchers revealing sub-surface soil-structure interactions. Examples include pile-installation behaviour and induced damaged (McCarel and Beard 1984, Alvarez-Borges et al. 2022), strain accumulations and shear band development in triaxial element tests (Desrues et al. 1996), the behaviour of laterally loaded piles (Otani et al. 2006) and the growth of new plant roots (Viggiani et al., 2015), to name a few. As the test is typically carried out outside a scanner bay, most applications of X-ray computed tomography

(CT) have been limited to post-test analysis or methods in which the position of the test structure is fixed in place. Therefore, there have been limited examples of scans under an active load (e.g., Sato et al., 2018, who developed a small-scale apparatus capable of studying axial and torsional pile behaviour). To overcome this limitation, a new multi-axis loading frame (the ICE-PICK apparatus) has been developed for operation within a lab-based CT. This has enabled the observations of various geotechnical phenomena via time-resolved radiography and in-test CT. In this paper, an overview of the frame construction and performance is provided, together with a demonstrative test performed during the ICE-PICK testing campaign. The test entailed the installation and multi-directional loading of a small-scale pile foundation in a low-density soft rock (calcarenite), paired with X-ray CT. It will be shown how the effects of installation lead to a radial damage zone surrounding the pile which influences the lateral performance of piles at low strain levels.

2 NEW APPARATUS

The multi-axis frame, in its current iteration (Figure 1) was designed and optimised to fulfil geometrical, weight and operational load and displacement constraints. Size and weight limits were dictated by the University of Dundee's SMART lab CT scanner, which resulted in a system with a height of 900 mm, a width/breadth of ~360 mm and weight of 50 kg.

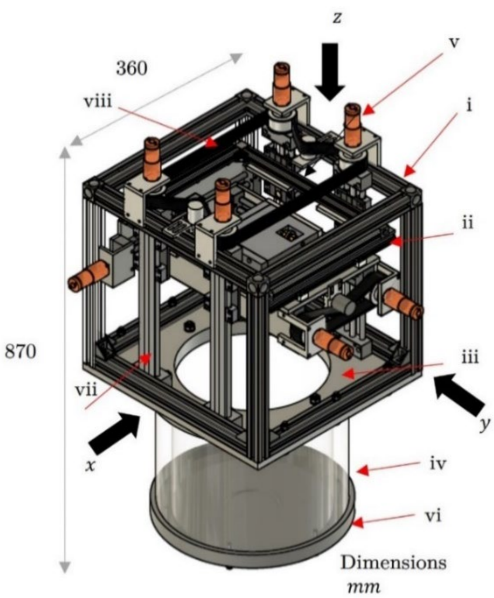

Figure 1: Multi-axis frame system in large chamber arrangement showing key components (i-vii)

The operational load and displacement values were dictated by the requirements of the ICE-PICK project and, therefore, the ability of the frame to install small-scale piles into soft rock (i.e., $\sigma_c < 4$ MPa). This led to a maximum vertical load capacity of 5 kN and a horizontal load of 500 N, as shown in Table 1. Further information may be found in Riccio et al. (2024b).

2.1 Materials and fabrication

Off-the-shelf parts were used to fabricate the main outer and inner frame structural components, as shown in Figure 1 (part i, ii). Referring to Figure 1, the inner and top/base plate (part iii/vi) were machined from 6061 Aluminium plates to achieve sufficient structural rigidity. Linear motion IGUS Drylin SLW guides for actuation were assembled on the vertical and horizontal loading axes (part v). The vertical axis motion was driven by 4No. MFA 1:264 DC motors (part v), whilst synchronicity of the linear guides was maintained via a timing system of steel-reinforced polymer belts, as also employed for the y direction (e.g., viii). The x direction was driven via 1No. 1:516 DC motor. The system currently accommodates two different chamber arrangements: a small and large diameter 120 mm and 300 mm, respectively, as shown in Figure 1 (part iv). Before construction, the suitability of the chosen materials and frame structure were assessed using FE analysis, undertaken in Fusion 360.

2.2 Control system and performance

The control system was capable of both displacement and load controlled test regimes, by means of an automatic tuning proportional-integral-derivative feedback control (PID) facilitated by LabView. Feedback utilised the minature Omega +/- 5 kN load cells at the connection within the rigid box and TF Connectivity Displacement reels which were stationed on each axis to measure global displacement. The operational frequency of the system was 50 Hz, to maintain a good PID feedback performance and adequate sensor sampling rate, to avoid aliasing artefacts, particularly in cyclic testing. System performance (Table 1) was assessed through various tests during the calibration of the PID control. For further information see Riccio et al. (2024b).

Table 1: System performance and measurement accuracy. *Where* $\boldsymbol{U}$ *is displacement range and* $\boldsymbol{u}$ is displacement rate.

System limit	z	x	y
U (mm)	120	100	100
Load (N)	5000	150-500	150-500
u (mm/s)	0.02-0.4	0.02-0.1	0.02-0.4
Cyclic freq. (Hz)	0.05-0.2	0.01-0.08	0.05-0.2
Load accuracy		0.25%	
U accuracy		0.2 %	

3 POTENTIAL USES AND EXAMPLES

The system has been used to carry out a number of small-scale tests, including model root push-over and inclined loading tests, as well as pile and CPT penetration tests. In this example, one test from the ICE-PICK testing campaign is provided, which consisted of approximately 25 individual open and close-ended pile and CPT tests undertaken in soft rock samples. These tests included full-installation processes (impact and continuous jacking), lateral (monotonic, 1-way, 2-way and partial 2-way) and axial (2-way) cases, as well as multi-directional lateral and vertical cases. More information on these multi-stage tests is provided in Riccio et al. (2024a). In this scope, a multi-directional test is described, which comprised both vertical and lateral cyclic conditions for assessment of load application on lateral performance, as discussed in the forthcoming section.

4 VERTICAL AND LATERAL CYCLIC PERFORMANCE OF PILES IN CALCARENITE

4.1 Materials and pile properties

The soft rock sample ($\sigma_c < 2$ MPa, $d_{50} = 86$ µm) consisted of a highly porous calcarenite rock which is present at several offshore wind farms (Ciantia et al., 2015; Palix & Lovera, 2020; Beemer et al. 2023). The cored soft rock sample (150 x Ø100 mm), was fully saturated and installed into the small chamber arrangement and restrained with a 10 mm band of self-levelling epoxy resin. The model pile foundation had a diameter (D) of 18.85 mm ($t_w = 0.91$ mm) and was machined from stainless steel, resulting in a flexural rigidity of $EI \approx 0.46$ kNm^2.

4.2 Test stages

The test was formed of two main stages, namely rapid jacked installation ($0 - 5.27\ z/D$) followed by lateral monotonic and cyclic lateral loading.

4.2.1 Installation stages

Installation was achieved by pulsing the z actuator in approximately 5 second increments and with a magnitude of 0.45 mm/s, maintaining quasi-drained conditions due to the hydraulic conductivity of the coarse-grained soft rock ($k_v \approx 10^{-4}$ m/s).

4.2.2 Lateral stages

After 5.27 z/D penetration, lateral monotonic and cyclic load tests were performed, acting on the pile head. The pile behaviour was assumed to be approximately that of a rigid body, as suggested by the relative stiffness approach defined in Abadie et al. (2019). An ultimate lateral load of $P_u = 355\ N$ was obtained from a separate monotonic lateral test, where P_u was defined by the lateral load at a pile head displacement equivalent to 0.1D (Cuéllar 2011). This was used to define the cyclic load amplitude (P_{max}), which was based upon the LeBlanc et al. (2010) cyclic characteristic parameters. In this case, a P_u was selected such that $\zeta_b \approx P_{max}/p_u \approx 0.30$, which was close to a typical pile fatigue limit as specified in Arshad & O'Kelly (2014). The cyclic frequency selected (0.06 Hz) was a little below the typical peak frequency of an average North-sea offshore wave, of approximately 0.106 Hz (Abadie et al. 2019) and with a loading bias of $\zeta_c = P_{min}/P_{max} = -1$ (i.e., full two-way); see LeBlanc et al. (2010). These characteristics were applied to the pile and paired with different initial vertical loads (F_z) ranging from 0 N to 800 N. Noting that slight offset in amplitude of the two-way cycle was observed and attributed to minor undershoot of the PID control system.

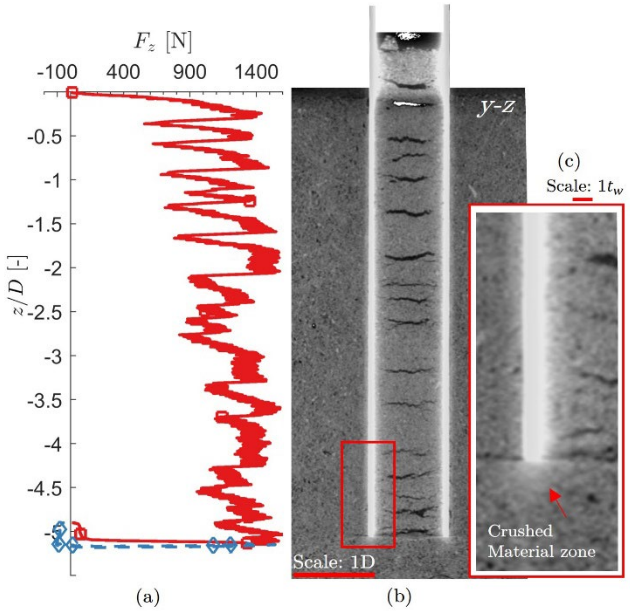

Figure 2: Quasi-impact jacked installation (a) Force-penetration and tension response (b) XCT Centre-slice in y-z plane through centre of penetrated pile. (c) Close-up of tip zone. Scan properties: frames per position (3141) acquired with an X-ray beam tension of 220 kV and current of 500 µA, D is diameter and t_w is pile wall thickness.

4.3 PILE JACKED INSTALLATION

The installation load-displacement curve, shown in Figure 2a, highlighted that the pile head force remained consistent throughout penetration, indicating full coring conditions.

However, minor stick-slip events, likely generated by the rapid jacking (i.e. negligible creep during the stick phase) were associated with local peaks (≈ 1300 N) and dips ($\approx 400-800$ N) of combined basal and shaft force. Ignoring the contribution from the shaft, local peak values roughly corresponded to the materials' intact yield stress in oedometric conditions assuming full base contact which was thought to be true upon the re-initiation of jacking ($\sigma_{oed} \cdot A_{base,eff} \approx 900$ N), where $A_{base,eff}$ considered the base area and apparent damage zone around the pile of 1-1.5 mm observed in Figure 2c. Post-installation uplift tests indicated a very low shaft contribution which degraded quickly during pullout. This was thought to be related to the materials' high porosity and limited lateral confinement after crushing.

4.4 POST INSTALLATION X-RAY CT OBSERVATIONS

The unplugged characteristics and stick-slip events highlighted above were confirmed by both the post-installation CT (see Figure 2b) and visual assessment of the pile plug (extracted after the test). These revealed a core content of assorted intact and crushed pieces, which was approximately 6.1 z/D in length (i.e., >5.30 z/D insertion, indicating dilation). The longer pieces of intact material coincided with the measured changes in the force-displacement response (see Figure 2a-b), further evidencing possible stick-slip events or local seperation of the dense plug during pauses in the jacking process, which enabled stress relaxation at the tip. The post-install CT highlighted a damage zone ahead of the pile that was concentrated around the tip zone, which was approximately equal to the wall thickness ($\approx 0.45-1$ mm), as shown in Figure 2b and c and confirmed with post-test destructive sample analysis. In general, the sample appeared minimally disturbed outwith the near-pile damage zone and both the interior and exterior of the pile, consistent with the behaviour of a fully-coring pile, as well with other existing datasets in which full coring conditions were observed (Alvarez-Borges et al. 2022).

4.5 LATERAL CYCLIC RESPONSE

4.5.1 Installation effects

The damage zone caused by pile installation appeared to affect the lateral performance. This is shown in the lateral cyclic stage where $F_z = 0$ (Figure 3a) which exhibited a sigmoid shaped response, typical of elasto-plastic hysteretic responses, characterised by low initial stiffness at low strain levels. This was further confirmed by the secant stiffness (K_{sec}) of the cyclic profiles (see Figure 3b).

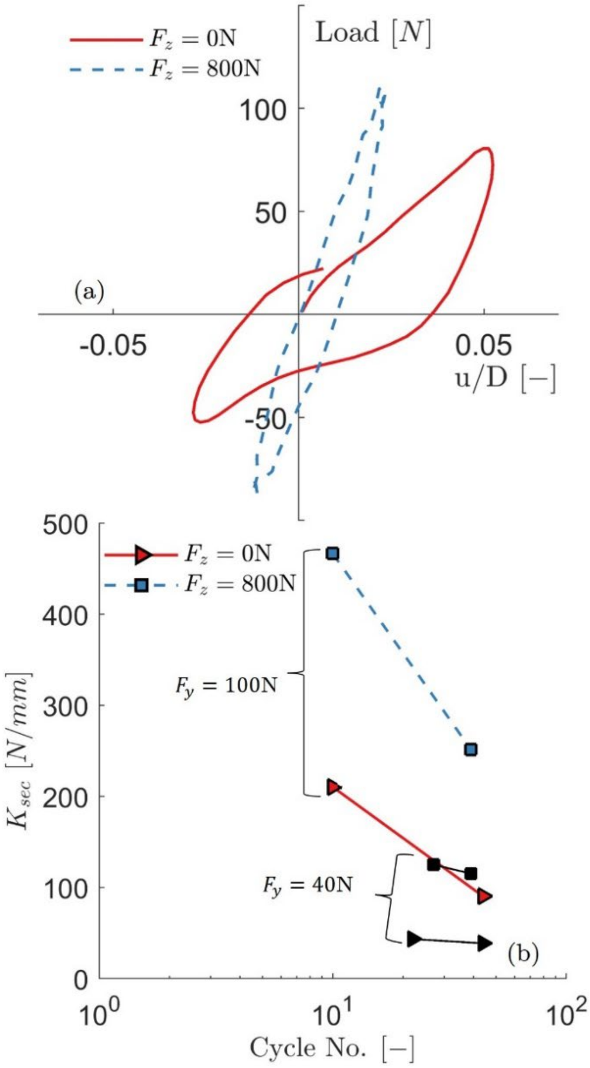

Figure 3: Cyclic response of flexible OE pile in calcarenite with increasing vertical force F_z (a) Force-displacement response (b) Secant stiffness

Herein, K_{sec} was defined as the ratio between lateral load ΔF_y and pile head displacement Δ_d during the positive load phase ($=\Delta F_y/\Delta_d$). At higher lateral displacements, K_{sec} was observed to increase by approximately $K_{sec,F_y=100} \approx K_{sec,F_y=40} \cdot 3$ in all cases. This stiffness increase appeared to occur when the pile had fully displaced beyond the low-stiffness damage zone, interacting with the stiffer intact and undamaged rock. More details can be found in Riccio et al. (2024a).

4.5.2 Effect of post-installation vertical load

Figure 3a clearly shows the influence of vertical load on the hysteretic loop shape of the laterally loaded pile. Increases in the load inclination appeared to reduce the lateral deflection of the pile, opposing the $P - \Delta$ effect (i.e., an increased vertical load leads to an increased bending moment and perceived pile deflection as was observed in $1g$ tests on granular non-cemented media reviewed by Li et al., 2020). This response was assumed to be associated with the mobilisation of a greater basal resistance due to higher confinement at the base, as well as the stiff surrounding media.

Due to the increased pile-soil interaction, stiffness degradation also appeared more marked with increased F_z due to rapid degradation of the basal resistance component (Riccio et al. 2024a). The authors assume that this was due to material yield ahead of the pile, which was thereafter liable to contractive effects and densification, as seen in oedometric and triaxial tests on intact samples (Leroueil and Vaughan 1990, Ciantia et al. 2018, Riccio et al. 2023).

A similar mechanism was envisaged to occur along the pile shaft, close to the pile tip, where high radial stresses are known to develop after installation (Jardine et al. 2023), further contributing to the increased residual displacement as the number of cycles increases and stress relaxation evolved. In these tests, the pile accumulated a residual displacement of approximately 0.6 mm in the $F_z = 0$ N case and approximately 0.2 mm in the $F_z = 800$ N case and which occurred over a relatively low-load cyclic response for <500 cycles. These characteristics highlighted the potential for pile instability directly related to the sensitive and complex mechanical behaviour of the soft calcarenite rock. Similar characteristics have been observed in field scale tests performed in rock mass by Ciavaglia et al. (2017) and Lovera et al. (2021), highlighting the importance of careful long-term design considerations that factor in the initial installation effects on the lateral performance of the pile.

5 CONCLUSION

In this short paper, some of the development of the ICE PICK testing apparatus has been described, including the system configuration, its performance, and the manufacturing process. The system has potential to perform a wide scope of small-scale tests, which was demonstrated by means of one of the ICE-PICK tests. This test utilised post-test CT scans to reveal some of the complexities of pile installation and lateral loading in soft calcarenite rock, at a small scale, highlighting the importance of careful design considerations for lateral pile performance in soft rock.

6 ACKNOWLEDGMENTS

This work is an output from the ICE-PICK project, funded by the EPSRC NIA grant EP/W00013X/1. The first author extends thanks to the EPSRC for support in funding and University of Dundee for resources essential to this doctoral research.

7 REFERENCES

Abadie, C.N., Byrne, B.W., and Houlsby, G.T. 2019. Rigid pile response to cyclic lateral loading: Laboratory tests. Geotechnique, 69(10): 863–876. doi:10.1680/jgeot.16.P.325.

Alvarez-Borges, F., Ahmed, S., Madhusudhan, B.N., and Richards, D. 2022. Investigation of pile penetration in calcareous soft rock using X-ray computed tomography. International Journal of Physical Modelling in Geotechnics, 22(1): 38–52. doi:10.1680/jphmg.20.00031.

Arshad, M., and O'Kelly, B.C. 2014. Development of a rig to study model pile behaviour under repeating lateral loads. International Journal of Physical Modelling in Geotechnics, 14(3): 54–66. doi:10.1680/ijpmg.13.00015.

Beemer, R., Foneseca, J., and Shaw, J. 2023. Non-invasive characterization of particle morphology of calcareous sands from Sao Tome & Principe. In IS-PORTO 2023: 8th International Symposium on Deformation Characteristics of Geomaterials, 3-6 Sep 2023, Porto, Portugal.

Ciantia, M., Lei, J., Monforte, L., Arroyo, M., and Gens, A. 2021. PFEM analysis of installation effects on axial performance of jacked piles in chalk. In 7th edition of the International Conference on Particle-based Methods. CIMNE.

Ciantia, M.O., Castellanza, R., and Fernandez-Merodo, J.A. 2018. A 3D Numerical Approach to Assess the Temporal Evolution of Settlement Damage to Buildings on Cavities Subject to Weathering. Rock Mechanics and Rock Engineering, 51(9): 2839–2862. Springer Vienna. doi:10.1007/s00603-018-1468-3.

Ciavaglia, F., Carey, J., and Diambra, A. 2017. Monotonic and cyclic lateral tests on driven piles in Chalk. Proceedings of the Institution of Civil Engineers: Geotechnical Engineering, 170(4): 353–366. doi:10.1680/jgeen.16.00113.

Cuéllar, V.P. 2011. Pile foundations for offshore wind turbines : numerical and experimental investigations on the behaviour under short- term and long-term cyclic loading. Dissertation,: 257.

Desrues, J., Chambon, R., Mokni, M., and Mazerolle, F. 1996. Void ratio evolution inside shear bands in triaxial sand specimens studied by computed tomography. Géotechnique, 46(3): 529–546. doi:10.1680/geot.1996.46.3.529.

Frick, D., and Achmus, M. 2021. A model test study on the parameters affecting the cyclic lateral response of monopile foundations for offshore wind turbines embedded in non-cohesive soils. European Academy of Wind Energy (Wind Energy Science Discussions), (November): 1–25.

Jardine, R.J., Buckley, R.M., Liu, T., Andolfsson, T., Byrne, B.W., Kontoe, S., McAdam, R.A., Schranz, F., and Vinck, K. 2023. The axial behaviour of piles driven in chalk. Géotechnique, 19(6): 1–45. doi:10.1680/jgeot.22.00041.

LeBlanc, C., Houlsby, G.T., and Byrne, B.W. 2010. Response of stiff piles in sand to long-term cyclic lateral loading. Geotechnique, 60(2): 79–90. doi:10.1680/geot.7.00196.

Lehane, B.M., and Gavin, K.G. 2001. Base Resistance of Jacked Pipe Piles in Sand. Journal of Geotechnical and Geoenvironmental Engineering, 127(6): 473–480. doi:10.1061/(asce)1090-0241(2001)127:6(473).

Leroueil, S., and Vaughan, P.R. 1990. The general and congruent effects of structure in natural soils and weak rocks. Géotechnique, 40(3): 467–488. doi:10.1680/geot.1990.40.3.467.

Li, Q., Prendergast, L.J., Askarinejad, A., and Gavin, K. 2020. Influence of vertical loading on behavior of laterally loaded foundation piles: A review. Journal of Marine Science and Engineering, 8(12): 1–18. doi:10.3390/jmse8121029.

Lovera, A., Ghabezloo, S., Sulem, J., Randolph, M.F., Kham, M., and Palix, E. 2021. Pile response to multi-directional lateral loading using P–y curves approach. Geotechnique, 71(4): 288–298. doi:10.1680/jgeot.18.P.297.

Mayoral, J.M., Pestana, J.M., and Seed, R.B. 2016. Multi-directional cyclic p-y curves for soft clays. Ocean Engineering, 115: 1–18. doi:10.1016/j.oceaneng.2016.01.033.

McCarel, S.C., and Beard, R.M. 1984. Laboratory Investigation on Piles in Calcareous Sediments. Naval Civil Engineering Lab Port Hueneme CA,.

Otani, J., Pham, K.D., and Sano, J. 2006. Investigation of failure patterns in sand due to laterally loaded pile using X-ray CT. Soils and Foundations, 46(4): 529–535. doi:10.3208/sandf.46.529.

Palix, E., and Lovera, A. 2020. Field testing for monopile to be installed in weak carbonated rock. ISFOG -21,: 1086–1095.

Peng, J.R., Clarke, B.G., and Rouainia, M. 2006. A device to cyclic lateral loaded model piles. Geotechnical Testing Journal, 29(4): 341–347. doi:10.1520/gtj100226.

Riccio, T., Ciantia, M., and Previtali, M. 2024a. 4D experimental investigation of installation effects on the axial and lateral response of piles in carbonate rock. Submission forthcoming,: 15.

Riccio, T., Previtali, M., Ciantia, M., and Brown, M. 2023. The Soft-Oedometer: A Simple Test to Calibrate Advanced Constitutive Models for CPT Simulations in Soft Rocks. In National Conference of the Researchers of Geotechnical Engineering. Springer Nature Switzerland, Cham. pp. 477–484.

Riccio, T., Romero, T., Mánica, M., Previtali, M., and Ciantia, M. 2024b. A 4D soil-structure interaction model testing apparatus. Geotechnical Testing Journal, 1(1): 1–12.

Roesen, H.R., Ibsen, L.B., and Andersen, L. V. 2013. Experimental testing of monopiles in sand subjected to one-way long-term cyclic lateral loading. 18th International Conference on Soil Mechanics and Geotechnical Engineering: Challenges and Innovations in Geotechnics, ICSMGE 2013, 3: 2391–2394.

Rudolph, C., and Grabe, J. 2014. Effect of variation of the loading direction on the displacement accumulation of large-diameter piles under cyclic lateral loading in sand. Canadian Geotechnical Journal, 51. doi:10.1139/cgj-2013-0438.

Sato, T., Onda, K., and Otani, J. 2018. Development of a new loading test apparatus for microfocus X-ray CT and its application to the investigation of soil behavior surrounding driven open-section piles. Soils and Foundations, 58(3): 776–785. Japanese Geotechnical Society. doi:10.1016/j.sandf.2018.03.004.

Su, D. 2012. Resistance of short, stiff piles to multidirectional lateral loadings. Geotechnical Testing Journal, 35(2). doi:10.1520/GTJ103840.

Viggiani, G., Andò, E., Takano, D., and Santamarina, J.C. 2015. Laboratory X-ray tomography: A valuable experimental tool for revealing processes in soils. Geotechnical Testing Journal, 38(1): 61–71. doi:10.1520/GTJ20140060.

Yuan, B., Xu, K., Wang, Y., Chen, R., and Luo, Q. 2017. Investigation of Deflection of a Laterally Loaded Pile and Soil Deformation Using the PIV Technique. 10(6): 1–9. doi:10.1061/(ASCE)GM.1943-5622.0000842.

Zheng, J., Previtali, M., Ciantia, M., and Knappett, J. 2023. Comparison of continuum (PFEM) and discrete (DEM) approaches for large insertion BVPs in soft rocks. In VIII International Conference on Particle-Based Methods. CIMNE, Milan. pp. 1–9.